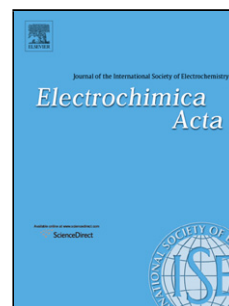# Accepted Manuscript

Title: Mechanically activated carbonized rayon fibers as an electrochemical supercapacitor in aqueous solutions

Authors: Milica Vujković, Ljiljana Matović, Jugoslav Krstić, Marija Stojmenović, Anelka Đukić, Biljana Babić, Slavko Mentus

Please cite this article as: Milica Vujković, Ljiljana Matović, Jugoslav Krstić, Marija Stojmenović, Anelka Đukić, Biljana Babić, Slavko Mentus, Mechanically activated carbonized rayon fibers as an electrochemical supercapacitor in aqueous solutions, Electrochimica Actahttp://dx.doi.org/10.1016/j.electacta.2017.06.018

This is a PDF file of an unedited manuscript that has been accepted for publication. As a service to our customers we are providing this early version of the manuscript. The manuscript will undergo copyediting, typesetting, and review of the resulting proof before it is published in its final form. Please note that during the production process errors may be discovered which could affect the content, and all legal disclaimers that apply to the journal pertain.

Mechanically activated carbonized rayon fibers as an electrochemical supercapacitor in aqueous solutions

Milica Vujković[1,*], Ljiljana Matović[2], Jugoslav Krstić[3], Marija Stojmenović[2], Anđelka Đukić[2], Biljana Babić[2], Slavko Mentus[1,4]

[1]*Faculty of Physical Chemistry, University of Belgrade, Studentski trg 12–16, 11158 Belgrade, Serbia*

[2]*Institute of Nuclear Sciences "Vinča", Mike Petrovica Alasa 12–14, 11001 Belgrade, University of Belgrade, Serbia*

[3]*University of Belgrade, Institute of Chemistry, Technology and Metallurgy, Department of Catalysis and Chemical Engineering, Njegoševa 12,11000 Belgrade, Serbia.*

[4]*Serbian Academy of Sciences and Arts, Knez Mihajlova 35, 11000 Belgrade, Serbia*

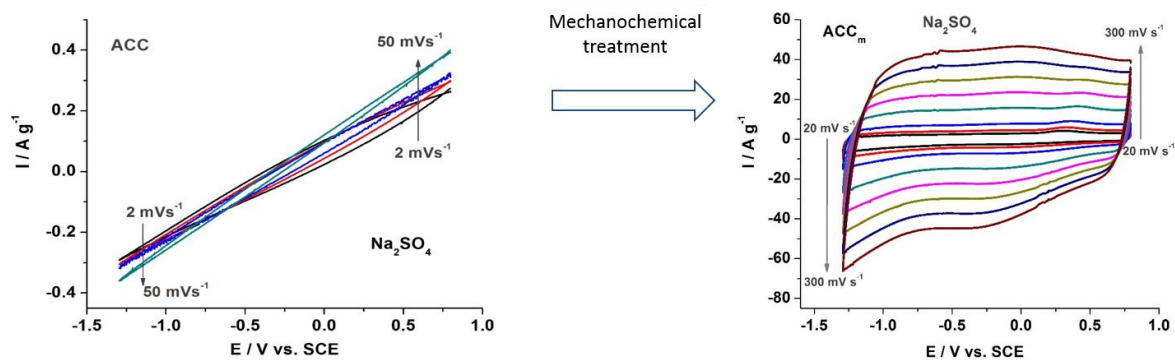*Corresponding author: Milica Vujković, PhD

University of Belgrade, Faculty of Physical Chemistry

Studentski trg 12–14, 11158 Belgrade, Serbia

E–mail address: milica.vujkovic@ffh.bg.ac.rs;

Tel.: +381 112187133; Fax: +381 11 340 8224

Graphical abstract

Highlights

- The carbonized rayon fibers were mechanochemically activated.

- High operating voltage of 2.1V achievable with aqueous electrolyte.

- Designed aqueous carbon capacitor delivers a very high energy density of 31 Wh kg^{-1}.

Abstract

The activated carbon cloth (ACC), obtained by chemical/physical activation of carbonized rayon fibers, was grinded in a ball mill and studied from the aspect of double layer capacitance. The changes in pore structure, morphology and acid/basic properties caused by ball milling were studied by means of N_2 adsorption/desorption, Fourier-transformed infrared spectrometry, Boehm's titration and Scanning Electron Microscopy. Both potentiodynamic and galvanostatic cycling were used to evaluate the double layer capacitance in three alkaline, acidic and neutral aqueous solutions (KOH, H_2SO_4 and Na_2SO_4). While double layer capacitance of original ACC was found to be negligible, ball milled material (ACCm) displayed capacitance in the range of supercapacitors. In order to explain this huge capacitance improvement, we found that ball milling substantially increased the concentration of lactone, phenolic and quinone groups on the surface. We suggest that these groups, through improved hydrophilicity, enable faster ion diffusion into carbon micropores. The energy density stored by double layer was highest in neutral sodium sulphate solution. Namely, operational voltage of ~2 V and double layer capacitance of 220 F g^{-1} at 1A g^{-1}, enable the energy density of ACCm/Na_2SO_4/ACCm capacitor of 31.7 Wh kg^{-1} at 2000 W kg^{-1}, much higher than that of commercial EDLC carbon capacitors. According to the here presented literature survey in a tabular form, the energy density of the studied sample is also higher from that of numerous thus far published aqueous carbon capacitors.

Keywords: carbon supercapacitor, mechanochemical activation, Na_2SO_4 aqueous electrolyte, high energy.

1. Introduction

The carbon-based supercapacitors in aqueous KOH and H_2SO_4 solutions may provide extremely high capacitance reaching 150-350 F g^{-1} [1-3]. Relatively low voltage window $\leq$ 1V available for capacitor charging/discharging processes in aqueous solutions present the main obstacle in their commercialization [3-6]. Ania et al. [4] found that commercial activated carbon as capacitor electrode material underwent the oxidation degradation in the periods of anodic polarization. Both acidic and alkaline aqueous solutions have been preferentially used as electrolytes in aqueous supercapacitors, displaying higher conductivity [7] and slower faradaic processes [8] in comparison to neutral solutions. Namely, capacitances measured in neutral aqueous electrolytic solutions, ranging 50 to 140 F g^{-1}, are generally lower from capacitances measured in either acidic or alkaline solutions [5, 7, 9-13].

Demarconnay et al. published a pioneering work [14] in which they described a very high voltage window of 2.4 V achievable in Na_2SO_4 solution with an activated carbon (AC) working electrode in a three-electrode cell. However, voltage interval of only 1.6 V was achievable in a symmetric two-electrode arrangement, with two AC electrodes. In this arrangement capacitance of 125 F g^{-1} at the rate of 1 A g^{-1} was measured, with displayed very slight fade on cycling. This study incited a rising interest for application of neutral aqueous electrolytes in carbon based capacitors [15-18]. Yang et al [17] showed that supercapacitors based on hydrated graphene film with neutral electrolyte solution can operate at the voltage of 1.8 V, providing the capacitance of $\sim$ 200 F g^{-1} at a rate of 1 A g^{-1}. Fic et al. [6] described a symmetric carbon capacitor operable at voltage close to 2.2 V using 1 mol dm^{-3} Li_2SO_4 solution as the electrolyte. For this supercapacitor only a slight capacity decrease from 140 F g^{-1} to 120 F g^{-1} was evidenced after even 15000 charging/discharging cycles.

Babel and Jurewicz [19] demonstrated that viscose rayon carbon fibers, chemically activated in hot KOH solution, provide very high capacitance of 340 F g^{-1} and 270 F g^{-1} in 4 mol dm^{-3} H_2SO_4 and 7 mol dm^{-3} KOH solutions, respectively. Milczarek et al. [20], for commercial activated carbon fiber cloth, surface enriched by oxygen, measured high capacitance of 161 F g^{-1} in sulfuric acidic solution, which even increased to 172 F g^{-1} by potentiostatic oxidation.

3

Ball milling process has been applied to modify the properties of various carbonaceous materials including carbon nanotubes (CNTs) [21-26], graphite [27,28] and activated carbon cloth [29]. For instance, ball milling, transformed CNT's into nanoparticles [21]. Figueireido et al. [25] developed a simple solvent-free method to obtain N-doped CNTs by ball milling of melamine or urea. The single-walled CNTs [23] and graphite [27], upon ball milling became capable of intercalating high amount of lithium ions. Mechanochemically treated microporous activated carbon cloth, obtained by simultaneous carbonization and CO_2-activation of viscose rayon cloth [29], may be used as effective adsorber of As (V) [30] and some other pollutant ions (zinc, cadmium mercury) [31] from aqueous solutions.

Having in mind the successful use of neutral aqueous solutions in carbon supercapacitors [14-18], and the possibility of activation of carbonized rayon fibers by ball milling [19, 30], in the present paper, we investigated the applicability of mechanochemically activated carbonised rayon fibers as electrodes of symmetrical supercapacitors with aqueous electrolyte solutions. To the best of our knowledge, this is the first study of mechanochemical modification of this abundant and cheap raw material for the use in the field of supercapacitors. A comparative study was performed in pH-different aqueous solutions, KOH_{aq}, H_2SO_{4aq} and Na_2SO_{4aq}. The results evidenced that mechanochemical modification significantly improved charge storage behavior. Namely, in neutral Na_2SO_4 solution, symmetric supercapacitor operable in a wide voltage interval of ~ 2V is realized, with an energy density being among the highest ones thus far reported for carbon supercapacitors with aqueous electrolyte.

2. Experimental section

The commercial rayon cloth (Viskoza, Loznica) impregnated by $ZnCl_2$ and NH_4Cl solutions, carbonized and simultaneously activated by CO_2, designated as ACC, [30] was used in this study. The cloth was transformed to carbon powder (ACCm) by milling in a Turbula Type 2TC mixer under air atmosphere. The milling process was performed in hardened steel vial with BPR fixed at 20:1 and milling time of 20h. A very fine powder was obtained. Similar procedure has been recently used in ref.[29]. However, in this study, before milling, we washed ACC sample with 0.1M HNO_3, to remove Zn-containing impurities used in activation procedure, when the surface was simultaneously subjected to a slight oxidation. The adsorption-desorption

isotherms of ACCm were measured by nitrogen adsorption at 77 K using a Sorptomatic 1990 Thermo Finnigan device. Prior to adsorption, the samples were degassed for 4 h at room temperature under vacuum, additionally 8h at 383 K and finally 12 h at 523 K at the same residual pressure. Various models [32-35] and appropriate software ADP Version 5.17 CE Instruments were used to analyse the obtained isotherms. The total pore volume (V_{tot}) was calculated applying the Gurevitsch's rule [32] at relative pressure p/p_0=0.95 (p and p_0 represent the equilibrium and saturation pressures of nitrogen at the temperature of adsorption). The specific surface area, S_{BET}, was calculated according to the Brunauer, Emmet, Teller method. The interval of p/p_0 for BET plot was selected using procedure proposed by J. Rouquerol at al. [33]. Micropore volumes were obtained using the t-plot method (V_{mic}-t), Dubinin-Radushkevic method (V_{mic}-DR) [34] and Horvath-Kawazoe method (V_{mic}-HK) [35]. Absorbance spectra were measured in the range of 4000-400 cm^{-1}, at 2 cm^{-1} resolution, using Nicolet 6700 FTIR spectrometer (Thermo Scientific). The KBr pellet technique was used. In order to disperse ACC in KBr and made pellet, the peace of ACC cloth was grinded by mortar and pestle. Since the fine powder of ACC was very difficult to get in such a way, Fourier transform infrared attenuated total reflection spectroscopy (FTIR-ATR) was also measured form both ACC and ACC$_m$ samples in order to check the reliability of all collected data. FTIR-ATR spectra were measured using FTIR-ATR spectrophotemeer Nicolet iS10 (Thermo Fisher Scientific). The amounts of acidic and basic surface functional groups were evaluated by Boehm's titrations method [36]. The morphology of samples was observed using the VEGA TS 5130, Tescan Scanning Electron Microscope.

Cyclic voltammetry was measured with a three-electrode cell by the Gamry device while the galvanostatic measurements were performed with a two-electrode cell by a battery Arbin cycler. The conventional configuration of the three-electrode cell was used, with a working electrode, platinum foil as a counter electrode and saturated calomel electrode as the reference electrode. The piece of ACC cloth was used directly as a working electrode while the ACCm electrode was made from the slurry which contained the ACCm powder. In fact, the slurry was made by mixing the N-methyl-2-pyrrolidone solution of the ACCm, carbon black and poly(vinylidene fluoride (85:10:5), followed by ultrasonication for 0.5h. After that, the slurry was coated uniformly, in the form of thin layer, to the conductive glass carbon (for three electrode

measurement) as well as to the stainless steel electrodes (for two electrode configuration). All electrodes were dried in an oven, under vacuum at 135°C, to evaporate pyrrolidone. The cyclovoltametric measurements were performed in the aqueous solutions of 6 M KOH, 1 M Na_2SO_4 and 1M H_2SO_4. Two stainless steel electrodes were constructed in the symmetrical configuration with a separator soaked by the electrolyte (1M Na_2SO_4) between them. The cell was cycled between 0 and 2V (and 2.1V) with various current from 1 A g^{-1} to 10 A g^{-1}. The galvanostatic measurements were done in the 1 mol dm^{-3} aqueous solution of Na_2SO_4 at a room temperature.

The specific capacitance of ACCm, C_s (F g^{-1}), from the cyclovoltametric measurements, were calculated according to the formula $C = (\int i \cdot V \cdot dV) / (m \cdot v \cdot \Delta V)$ where i is the measured current response, V is the potential, m is the mass of the exposed material to the electrolyte, v is the applied scan rate and ΔV is the used potential window.

The specific capacitance of ACCm, from the galvanostatic measurements, were calculated according to the formula C_{spec} (F g^{-1}) = 2 i Δt / (ΔU x m) where m is the mass of one electrode, i is the applied current, Δt is discharge time and ΔU is the applied voltage interval. The energy density of ACCm/ACCm capacitor, based on the total mass of electrode, was calculated according to the formula $E = 1/8 \ C_{spec}\Delta \ U^2$ while the average power density was calculated by using the equation P=E/Δt.

3. Results and discussion

3.1. Surface characterization

The changes in the surface chemistry and morphology of carbon cloth, caused by the mechanochemical milling treatment, were studied.

Nitrogen adsorption−desorption isotherms of ACC and ACCm samples are presented in Fig.1, while the calculated textural parameters are given in Table 1.

Figure 1

6

The shape of obtained isotherms, according to the IUPAC classification, is Type 1 which is typical for microporous materials. Slight difference between isotherms can be observed in a "knee region", as well as in the region of relative pressure which corresponds to mesoporous area. The somewhat pronounced slope of isotherm of milled sample was observed. However, microporous nature of both materials is obvious due to: sharp increase of V_{ads} in low relative pressures, existence of long flat plateau and complete reversibility of desorption brunch. Very high developed microporous surface area is observed for both samples, which actually originates from the chemical activation during ACC manufacturing. Although CO_2 adsorption is more advantageous in determination of surface area of microporous carbons by BET procedure [37] the results obtained by N_2 adsorption prevail in the literature, and are used in this study, too. The S_{BET} values of ACC and ACCm amount to 1028 $m^2 g^{-1}$ and 1340 $m^2 g^{-1}$, respectively. The increase of the carbon specific surface area after milling process, has already been observed for milled CNTs [24-26]. It can be clearly seen from Table 1 that milling process of ACC caused increase of all textural parameters including specific surface area (+30%) and total pore volume (+38%). The micropore volume, for all applied calculation methods (t-plot, Horvath-Kawazoe and Dubinin-Raduskevich), also increases and reaches values above 0.5 cm^3/g. In addition, the broader micropore size distribution is noticeable according to calculation based on the Horvath-Kawazoe model, as can be seen in Fig.1b.

Table 1

The changes in surface ACC chemistry, induced by milling process in the air atmosphere, are examined by both Boehm's titration and FTIR techniques.

The results of Boehm's method are listed in Table 2. It can be seen that unmodified ACC sample has a significantly higher number of acidic groups at the surface (2.51 mmol g^{-1}) in comparison to the number of basic groups (0.2493 mmol g^{-1}). It reveals the acidic character of ACC. The phenolyc acidic groups dominate at the ACC surface, amounting to 95% of the total content of acidic groups. The carboxyl groups are present in a small amount (4.7% of the total content of acidic groups). A small fraction of lactonic groups (less than 0.3%) was also observed.

The increase of both acidic (2.5093→3.5313) and basic (0.2493→0.7933) groups upon applied treatment is clearly evidenced (Table. 2). One can see that the ball milling process of ACC reduces its acidic character by increasing the content of basic groups (~3.2 times higher). The increase of acidic groups (~1.4 times higher) is the result of the significant increase in the number of phenolic groups (2.3846→3.4106) and the small increase of the lactonic groups (0.0074→ 0.0094). The increase of the phenolic and lactonic groups has already been observed in the activation process of carbon by using either nitric acid or hot dry air [38].

Table 2

FTIR spectra of both ACC and ACCm samples are shown in Figure 2a. The pronounced peaks on FTIR spectrum of ACCm, contrary to the FTIR spectrum of ACC (which show high signal to noise ratio), appear as a consequence of increased number of different oxygen containing groups (-OH, C-O, C=O). As can be seen from the Fig.2a, the three characteristic bands of ACCm, centered at ~1720 cm^{-1}, ~1584 cm^{-1} and ~1217 cm^{-1}, became intensive after milling treatment. The appearance of these bands is typical for oxidation treatment of graphitized carbon cloth [39,40]. Due to the interactions of surface groups as well as coupling of the close vibrations modes, the assignment of carbon FTIR bands, by various authors, has been interpreted equivocally [41]. Generally, [39, 42] the assigned bands of ACCm belong to the stretching vibration of C=O in anhydride, lactone, esters and/or carboxyl acid (~1720 cm^{-1}), quinone and C=C structure (~1584 cm^{-1}) , C-O stretching and O-H bend/strech modes (~ 1217 cm^{-1}). Since the aldehydes and OH functional groups of ACC (originating from cellulose molecules) can be easily oxidized, up to the carboxylic groups, the increase of COOH groups upon applied treatment could be realistically expected [43]. However, Boehm's method shows that the amount of carboxylic groups is not increased by the applied milling process. One can notice that the position of 1740 cm^{-1} band shifts towards the lower wave number (1720 cm^{-1}) after the oxidation treatment. The formation of lactone groups causes this low-frequency shifting [44]. The intensity of both 1584 cm^{-1} and 1217 cm^{-1} assigned bands was significantly increased by the milling process, thus confirming the increased amount of quinone (evidenced by cyclic voltammetry, as shown below) and phenolic groups, respectively. All these observations are in accordance with

the Boehm's titration results. The shifting vibration mode from 1560 cm^{-1} to 1584 cm^{-1}, upon milling process, indicates a high number of coupled vibrations of C=O with C=C in ACCm.

Figure 2

Powdered form of ACC sample was made, with the mortar and pestle, in order to make KBr pastille for FTIR measurement. Since the homogeneity of the ACC powder was very difficult to obtain in this way, FTIR-ATR spectra of pristine samples were also measured. The same trend, as interpreted above, was observed thus confirming the reliability of spectra shown in Figure 2a. Namely, the similar ratio of signal to noise in the ATR spectra, between ACC sample (the piece of carbon cloth) and ACC powder (milled with the mortar and pestle), was obtained. It confirms the influence of the ball-milling process to the increased intensity of FTIR bands. Additionally, the ball milling provides a very fine ACCm powder that can be easily and homogeneously dispersed in the pyrolidone solvent. It's particle size distribution, determined from the SEM picture, shown as an inset in Fig 2, indicates the dominance of particles of < 0.5 micrometer in diameter.

The oxygen-containing groups, induced by mechanochemical milling in the air atmosphere, contribute to the better wettability of cloth sample.

Fig. 2 also shows the SEM microgprahs of ACC and ACCm samples. The breakage of ACC cylindrical micrometer fibers (Fig.2b) into irregular shape particles (Fig.2d), with decrease of particle sizes, was observed on SEM micrographs.

3.2. Capacitance properties in pH-different electrolytes

The cyclic voltamograms of ACC and ACC$_m$, are measured in three aqueous electrolytes with different pH (KOH, H$_2$SO$_4$ and Na$_2$SO$_4$), at various scan rates, in the appropriate voltage stability window, as shown in Fig. 3.

Figure 3

According to Fig.3 (a-c), a poor charge accumulation in ACC, in spite of its highly developed surface area, was observed in all electrolytes. The reason may be sought in small mean pore diameter, which, according to the BET measurements (Fig 1a), lies preferably below 1 nm. With this pore dimensions and a monolith appearance of the ACM, the permeability for hydrated ions, responsible for double layer capacitance, as discussed formerly by Chmiola et al. [45] and Gryglewicz et al. [46], is restricted to a rather small depth below the external surface. After pulverization, the pore exposure toward electrolyte increases drastically, and much higher fraction of the real surface area becomes accessible to electrolyte, Fig 3 (d-f). In addition, the charge storage decreases with the decrease in pH value. This is due to the acidic character of ACC cloth. On contrary, the modified ACC cloth delivers a very high charge storage capability in all electrolytes. The gradual increase of the scan rates up to 300 mV s^{-1} doesn't change the overall shape of CV curves indicating the excellent capacitance behavior of the milled sample. The pulverization of ACC fibers upon milling treatment (Fig.2) makes the path for ions and electrons through the electrode shorter and enables faster processes at the ACCm/electrolyte interface.

The redox peaks, superimposed to a box-like curve shape, are characteristic of CVs of milled sample in all aqueous electrolytes. They present the contribution of pseudocapacitance, and correspond to the change in oxidation state of surface groups. In the CVs of ACCm recorded in acidic solution, the redox peaks are typical of oxygen-containing carbons, and are mainly attributed to the quinone/hydroquinone reactions [8,47,48, 49]. Their highest intensity in acidic solution is consistent with the fact that quinone/hydroquinone redox reaction includes the participation of H$^+$ ions Following the literature, the assignment of faradaic reactions in alkaline solutions is not clearly established, while the faradaic reactions, in the neutral solution, are rarely observed [5, 13]. CVs of ACCm in Na$_2$SO$_4$, measured in different voltage intervals at the same scan rate (Fig. 4), indicate that the double layer of ACCm in Na$_2$SO$_4$ can be formed not only through the pure electrostatic adsorption of ions but also via faradaic reactions. Namely, redox peaks of ACCm positioned at -0.03/-0.08 V vs. SCE (20 mV s^{-1}) are clearly visible in the stable potential window of Na$_2$SO$_4$ (from -0.8 to -0.8 V vs. SCE), as shown in Fig.4. The fact that, relative to the peaks registered in acidic solution, they are shifted in cathodic direction, i.e. display pH dependence as observed in [50], makes reasonable the assumption that these peaks originate also from the quinone/hydroquninone reactions.

10

When the cut-off potential of CV measured in Na_2SO_4 at 20 mV s^{-1} was extended towards the deeper negative values, an additional anodic peak arises, which corresponds to the oxidation of stored hydrogen. The coverage of the surface by adsorbed hydrogen shifts the limiting value of negative polarization (limited by gaseous hydrogen evolution) and enables the increase of operating voltage of ACC_m.

Figure 4

The CVs of ACCm, measured in three different aqueous electrolytes, are shown in a comparable manner in Fig.5a. The overlapping of CV curves during the five cycles indicates the reproducible capacitance behavior of the sample. ACCm stores a comparable amount of charge at both negative and positive potentials, enabling to make symmetric capacitor using the suitable electrolyte such as is Na_2SO_4. Nevertheless, for higher scan rates ranging from 50 to 300 mV s^{-1}, the capacitance of ACCm measured in neutral solution (since the surface under the peak is normalized by the voltage interval) is somewhat smaller than that measured in either acidic or alkaline solution (Fig.5b). For lower scan rates, the capacity of ACCm in neutral and acidic solution is similar, while its value, in alkaline solution, is somewhat lower. The similar capacitance, close to the value of 140 F g^{-1}, was obtained in all electrolytes, at a scan rate of 50 mV s^{-1} (Fig.5b). Having in mind all said above, and fact that the operating voltage in neutral electrolyte is twice higher than the one in either acidic or alkaline solution, the sodium sulfate solution can be regarded as the most promising electrolyte for ACCm capacitor, less corrosive properties being an additional advantage.

The specific capacitance of ACCm in Na_2SO_{4aq} is pretty high at all observed scan rates. Its value ranged 130-160 F g^{-1} for the scan rate range 20 - 300 mV s^{-1}. At a very high scan rate of 300 mV s^{-1}, the cathodic capacitance was found to be 163.4 F g^{-1}, 133.1 F g^{-1} and 162.1 F g^{-1} while the anodic capacitance was found to be to 162.4 F g^{-1}, 131.1 F g^{-1} and 161.6 F g^{-1}, in KOH, H_2SO_4 and Na_2SO_4 solutions, respectively. The comparison to the available literature concerning the capacitance of various carbons in neutral aqueous electrolytes, in the same three-electrode configuration, [5, 7, 9, 10, 12, 51, 52], shows that the capacitance of ACCm belongs to the highest ones.

11

Figure 5

3.3. The study of pseudocapacitance of carbon/electrolyte boundary by complex impedance mesurements

The coupled faradaic and double layer charge storage on the interface ACCm/aqueous electrolyte solution, is clearly visible throughout the whole pH range. In order to understand these processes more deeply, impedance measurements were performed. Figure 6 shows the Nyquist diagrams of ACCm, in the examined aqueous electrolytes, at different bias potentials. The potentials for KOH and H_2SO_4 were chosen in such a way that they corresponded to the peaks of faradaic reactions (- 0.8V vs. SCE and ~0.27V vs. SCE, respectively). For the sake of comparison, the impedance of ACCm in Na_2SO_4 was also measured at these potentials. Although the faradaic reactions are regarded to be responsible for deviation of the low-frequency Nyquist line from the y-axis, a very small slope of this line was observed for ACCm in all electrolytes. It indicates an excellent capacitance behavior of the sample.

Figure 6

The high frequency intercept with the real axis, (Re), , as well as the estimated radius of the high frequency semicircle, i.e., the charge transfer (Rct), can be read directly from the measured Nyquist diagrams. R_e values amounted to ~ 0.5 Ω, ~ 0.9 Ω and ~2.1 Ω while the Rct values were estimated to be ~ 0.16 Ω, ~ 0.29 Ω and ~1 Ω for KOH, H_2SO_4 and Na_2SO_4, respectively. The R_{ct} value, measured in Na_2SO_4, is higher than the one measured in either alkaline or acidic solution, which indicates the coupling of mass transfer and charge transfer discussed by de Levie et al [53].

The transition frequency values can be also estimated from the impedance diagrams. The first transition frequency (f_{ct}), corresponding to the transition from the charge transfer (high frequency region) to diffusion region (middle frequency region), was estimated to be ~193 Hz (KOH), ~100 Hz (H_2SO_4) and $\sim$ 27 Hz (Na_2SO_4). The second frequency transition (f_w), corresponding to the transition from the diffusion region to capacitive region, amounted to 5.2

12

Hz, 2.7 Hz and 1.39 Hz, respectively. Also, the resistance values, obtained by the intercept of the low-frequency line with the real axis, were found to be approximately 0.77 Ω, 1.37 Ω and 3.78 Ω, respectively. One can see that all these parameters are in agreement with the rate capability of ACC_m, derived from cyclic voltammetry (see Fig.5).

The impedance diagrams of ACC_m, obtained at two potentials such as -0.8 V and 0.27 V vs. SCE in Na_2SO_4 solution are mutually similar. The small difference exists only in the low frequency region due to the contribution of hydrogen evolution at negative potential.

In our previous paper [54], we focused on some unresolved issues regarding the charge storage mechanism on carbon surfaces. The question was whether the negative cathodic slope of cyclovoltammograms, followed by an anodic hump, could be attributed either to the ions' retardation into pores or to the existence of O and/or N groups at the carbon surface. In principle, the synergy of the double layer with the faradaic process results in the complexity of the charge storage mechanism. We suggest that the CV deviation of the plane tree seed derived carbon (AC) is probably caused by the kinetic effects rather than the pseudo-capacitance influence. Here, we would like to pay attention to one interesting example which illustrates the difference between the double layer capacitance (AC sample reported in ref. [54]) and pseudocapacitance (ACC_m sample) of carbon. Fig. 7a shows comparative CVs of these samples, measured in KOH, within the water stability interval, at a common scan rate of 20 mV s^{-1}. In both cases, the distortion of CV curves (slope in Fig.7a) toward the negative potentials was observed, which probably corresponds to the retardation of ions motion into pores.

Figure 7

For ACC_m sample, the current humps (as broad peaks), superimposed to double layer current in both scan directions, can also be observed. These current bulges are related to the redox behavior of oxygen groups at the ACCm surface. In a different manner, the only anodic hump in CV of AC can be recognized in Fig.7a, which can be the consequence of the CV symmetry maintaining. In other words, the change in the oxidation state of surface elements over the whole applied voltage interval, which is typical for pseudocapacitance, is clearly recognized

in the CV of ACCm. The higher capacitance values of ACC_m than those of AC, at moderate scan rate, (Fig.7a) can be attributed to the contribution of pseudocapacitance

The difference in the charge storage between these two samples can be also seen in their coulombic efficiency. The coulombic efficiency, expressed as the ratio of cathodic and anodic capacity, amounted to ~100 % for AC and 98.3 % for ACCm. The existence of activation energy for surface faradaic process, relative to the barrier-less ion adsorption, results in slightly lower utilization of ACCm accumulated surface charge. Still, this difference is not too high due to the very fast redox processes of ACCm.

The pseudocapacitance behavior in CVs of ACCm can be recognized by shifting the positive "cut-off" potential toward positive values (Fig.7b). The electrochemical oxidation of carbon surface happens during the oxygen evolution reaction (OER), while the attached oxygen groups become reduced in the reverse cathodic scan. By looking at the Fig.7b, one can notice that the cathodic peak (which corresponds to the reduction of formed oxygen groups), increases over the whole voltage interval, thus proving the typical pseudocapacitance behavior.

3.4. High energy performance of neutral ACCm capacitor

Cyclic Voltammetry was used to evaluate the capacitance of ACC_m in three pH-different aqueous electrolytes such as KOH, Na_2SO_4 and H_2SO_4. The ACC_m was found to be applicable as a capacitor in any electrolytes' pH range. However, if all scan rates were taken into consideration (Fig. 5b), it could be said that the capacitance of ACCm in Na_2SO_4 was in range to those measured in KOH and H_2SO_4. Since the operating voltage in the Na_2SO_4 is two times higher than in other two electrolytes, the material was found to be the most promising for the neutral aqueous capacitors. Besides, the neutral aqueous capacitors are more environmentally friendly and safe than those which use either acidic or alkaline aqueous solution. Therefore, the galvanostatic measurements of ACCm are only performed in the neutral aqueous solution.

The galvanostatic curves of ACC_m, measured in Na_2SO_4, (Fig.8a) indicate that the material was capable to withstand a high voltage of 2 V, lacking water decomposition during

14

cycling. The specific capacitances, calculated from the galvanostatic curves, in relation to the current density, are shown in Fig. 8b. The initial specific discharge capacitance in F g^{-1} amounted to ~ 226 F g^{-1}, ~167 F g^{-1}, ~151 F g^{-1}, 133 F g^{-1}, 106 F g^{-1} at 1 A g^{-1}, 2 A g^{-1}, 3 A g^{-1}, 5 A g^{-1} and 10 A g^{-1}, respectively. After sequential measurements at various current rates, the capacitance was even enhanced for ~ 20 mAh g^{-1}. The measured capacitances exceed the values of other carbons in neutral aqueous electrolytes [5,11,14,17,52]. The upper voltage limits for very high currents (> 3 A g^{-1}) could be prolonged up to 2.1 V (Fig. 8c). Inset in Fig. 8c compares the capacitance values obtained within voltage window of 2 and 2.1V for 3 A g^{-1}, 5 A g^{-1} and 10 A g^{-1}. The similar values were observed. Good cyclic stability, after 1000 charge/discharge cycles, was demonstrated even at 2.1 V with a current density of 10 A g^{-1} (Fig. 8d). One can say that this material successfully withstood the surface oxidation during cycling in Na$_2$SO$_4$ solution equilibrated with air, at very high potentials, contrary to the capacitance deterioration on cycling at even lower voltages [4].

The maximal energy density, that can be stored/released by the ACCm/Na$_2$SO$_4$/ACCm capacitor cell, was found to be ~ 31.7 Wh kg^{-1}, ~ 23.4 Wh kg^{-1} and ~ 16.8 Wh kg^{-1} at a power density of ~2000 W kg^{-1} (1 A g^{-1}), ~5245 W kg^{-1} (5 A g^{-1}) and ~10497 W kg^{-1} (10 A g^{-1}), respectively. These values of are much higher than those provided by both commercially available carbon capacitors (using organic electrolytes), ranging from 5 to 10 Wh kg^{-1} [6, 53], and numerous aqueous carbon capacitors [14, 18, 55-59]. Namely, the energy density of ACCm/Na$_2$SO$_4$/ACCm capacitor was 3-5 times higher or more than 10 times higher than that of some other carbon capacitors [56-59]. In table 3, the values of energy and power density obtained in this work were compared to the values published in other papers [18, 56-68], for the capacitors of the same category (symmetric carbon electrodes).

Figure 8

Superiority of two-electrode ACCm capacitor in comparison to published ones can easily be seen. Wang et al. [18] reported symmetric supercapacitor, using flower-like and hierarchical porous carbon (FHPC) electrode, which delivered a very high energy density of 15.9 Wh kg^{-1} at a power density of 317.5 W kg^{-1}, operating in the voltage range of 0–1.8 V, in 1 mol dm^{-3} Na$_2$SO$_4$. These authors emphasized that the performances of FHPC capacitor are highly comparable to those of previously reported carbon capacitors. Here, the energy density is about 50% higher

15

from the one of a FHPC capacitors, at a significantly higher power density. These facts demonstrate the remarkable performance of the presented environmentally friendly and low cost 2V-carbon capacitor.

Table 3

4. Conclusions

The mechanochemical activation of viscose rayon carbon cloth was found to be an effective way for remarkable improvement of its charge storage behavior. This is a way to obtain cheap electrode material for energy rich eco-friendly and low-cost carbon supercapacitors. Collapse of cylindrical shaped microporous fibers together with the introduction of large amount of mainly basic character surface oxygen groups and increase in the surface area (from 1028 to 1340 m^2 g^{-1}) arose upon milling. The mecahnochemically activated carbon cloth (ACC_m) was found to be applicable in any pH range of aqueous electrolyte i.e. in KOH, H_2SO_4 and Na_2SO_4 aqueous solution. The charge separation, together with the pseudo-capacitance reactions, provides the high current capability of modified carbon (ACC_m) in three pH-different aqueous solutions. At a scan rate of 100 mV s^{-1}, the cathodic and anodic capacitance of ACCm amounted to 159.5 F g^{-1} and 157.97 F g^{-1} in KOH, 146.81 F g^{-1} and 143.36 F g^{-1} in Na_2SO_4, and 165.83 F g^{-1} and 165.8 F g^{-1} in H_2SO_4 solutions, respectively. Due to the highest operating voltage, Na_2SO_4 was found to be the most perspective electrolyte for assembly the ACC_m carbon capacitor. When operated at a very high voltage interval of ~2V, the $ACC_m/Na_2SO_4/ACC_m$ cell delivers a high and stable capacitance of ~220 F g^{-1} and ~120 F g^{-1} at 1A g^{-1} and 10 A g^{-1}, respectively. Consequently, a high energy density of the ACC_m two-electrode cell, amounting to 31.7 Wh kg^{-1} at a current density of 1 A g^{-1}, was demonstrated, making this "neutral" carbon capacitor superior when compared to the energy density (5-10 Wh kg^{-1}) of commercial carbon capacitors.

5. References:

[1] J. Yan, Q. Wang, T. Wei, Z. Fan, Recent Advances in Design and Fabrication of Electrochemical Supercapacitors with High Energy Densities, Adv. Energy. Mater. 4 (2014) 1300816 (1-43).

[2] B. Chang, Y. Wang, K. Pei, S. Yang, X. Dong, $ZnCl_2$-activated porous carbon sphere with high surface area and superior mesoporous structure as an efficient supercapacitor electrode, RSC Adv. 4 (2014) 40546- 40552.

[3] N. Gavrilov, I. Pašti, M. Vujković, G. Ćirić-Marjanović, J. S, S. Mentus, High performance charge storage by N-containing nanostructured carbon derived from polyaniline, Carbon 50 (2012) 3915-3927.

[4] C.O. Ania, V. Khomenko, E. Raymundo–Pinero, J.B. Parra, F. Beguin, The Large Electrochemical Capacitance of Microporous Doped Carbon obtained by Using a Zeolite template. Adv. Funct. Mater. 17 (2007) 1828–1836.

[5] M.P. Bichat, E. Raymundo–Piñero, F. Béguin, High voltage supercapacitor built with seaweed carbons in neutral aqueous electrolyte, Carbon 48 (2010) 4351-4361.

[6] K. Fic, G. Lota, M. Meller, E. Frackowiak, Novel insight into neutral medium as electrolyte for high-voltage supercapacitors, Energ. Environ. Sci. 5 (2012) 5842–5850.

[7] X. Zhang, X. Wang, L. Jiang, H. Wu, C. Wu, J. Su, Effect of aqueous electrolytes on the electrochemical behaviour of supercapacitors based on hierarchically porous carbons, J. Power Sources 216 (2012) 290–296.

[8] H. A. Andreas, B.E. Conway, Examination of the double-layer capacitance of an high specific-area C-cloth electrode as titrated from acidic to alkaline pHs, Electrochim. Acta 51 (2006) 6510-6520.

[9] C.C. Hu, C.C. Wang, F.C. Wu, R.L. Tseng, Characterization of pistachio shell-derived carbons activated by a combination of KOH and CO_2 for electric double-layer capacitance, Electrochim. Acta 52 (2007) 2498–2505.

[10] H. Konno, T. Ito, M. Ushiro, K. Fushimi, K. Azumi, High capacitance B/C/N composites for capacitor electrodes synthesized by a simple method., J Power Sources 195 (2010) 1739-1746.

[11] D. Hulicova, J. Yamashita, Y. Soneda, H. Hatori, M. Kodama, Supercapacitors prepared from melamine-based carbon, Chem. Mater. 17 (2005) 1241-1247.

[12] Y. J. Oh, J.J. Yoo, Y. II Kim, J. K. Yoon, H.N. Yoon, J.-H. Kim, S.B. Park, Oxygen functional groups and electrochemical capacitive behavior of incompletely reduced graphene oxides as a thin-film electrode of supercapacitor, Electrochim. Acta 116 (2014) 118-128.

[13] M. Stojmenović, M. Vujković, Lj. Matović, J. Krstić, A. Đukić, V. Dodevski, S. M. Živković, S. Mentus, Complex investigation on charge storage behavior of microporous carbon synthesized by zeolite template, Micropor. Mesopor. Mater. 228 (2016) 94-106.

[14] L. Demarconnay, E. Raymundo–Piñero, F. Béguin, A Symmetric carbon/carbon supercapacitor operating at 1.6V by using a neutral aqueous solution, Electrochem. Commun. 12 (2010) 1275- 1278.

[15] V. Subramanian, C. Luo, A.M. Stephan, K. S. Nahm, S. Thomas, B. Wei, Supercapacitors from Activated Carbon Derived from Banana Fibers, J. Phys. Chem. C 111 (2007) 7527-7531.

[16] Q. Gao, L. Demarconnay, E. Raymundo–Piñero, F. Béguin, Exploring the large voltage range of carbon/carbon supercapacitors in aqueous lithium sulfate solution electrolyte. Energ. Environ. Sci. 5 (2012) 9611–9617.

[17] X. Yang, Y.S. He, G. Jiang, X.-Z. Liao, Z.-F. Ma, High voltage supercapacitors using hydrated graphene film in a neutral aqueous electrolyte, Electrochem. Commun. 13 (2011) 1166–1169.

[18] Q. Wang, J. Yan, Y. Wang, T. Wei, M. Zhang, X. Jing, Z. Fan, Three-dimensional flower-like and hierarchical porous carbon materials as high-rate performance electrodes for supercapacitors, Carbon 67 (2014) 119-127.

[19] K. Babel, K. Jurewicz, KOH activated carbon fabrics as supercapacitor material, J. Phys. Chem. Solids. 65 (2004) 275-280.

[20] G. Milczarek, A. Ciszewski, I. Stepniak, Oxygen-doped activated fiber cloth as electrode material for electrochemical capacitor. J. Power Sources 196 (2011) 7882-7885.

[21] Y.B. Li, B.Q. Wei, J. Liang Q.Yu, D.H. Wu, Transformation of carbon nanotubes to nanoparticles by ball milling process, Carbon 37 (1999) 493-497.

[22] R.P.Rocha, O.S.G.P. Soares, J.L. Figueiredo, M.F.R. Pereira, Tuning CNT properties for Metal-Free Environmental Catalytic Appliations, C (Journal of Carbon Research) 2 (2016) Art. No 17; doi:10.3390/c2030017.

[23] B. Gao, C. Bower, J.D. Lorentzen, L. Fleming, A. Kleinhammes, X.P. Tang, L.E.McNeil, Y. Wu, O.Zhou, Enhanced saturation lithium composition in ball-milled single-walled carbon nanoutbes, Chem. Phys. Lett. 327 (2000) 69-75.

[24] I.Z. Papp, G. Kozma, R. Puskás, T. Simon, Z. Kónya, A. Kukovecz, Effect of planetary ball milling process of multiwall carbon nanotubes, Adsorption 19 (2013) 687-694.

[25] O.S.G.P. Soares, R.P.Rocha, A.G. Gonçalves, J.L. Figueiredo, J.J.M., Órfão, M.F.R. Pereira, Easy method to prepare N-doped carbon nanotube by ball milling, Carbon 91(2015) 114-121.

[26] N. Pierard, A. Fonseca A, J.-F. Colomer, C Bossuot, J.-M. Benoit, G. Van Tendeloo, J.-P. Pirard, Ball milling effect on the structure of single-wall carbon nanotubes, Carbon 42 (8-9) 2004 1691–1697.

[27] C.S. Wang, G.T. Wu, W.Z.Li, Lithium insertion in ball-milled graphite, J. Power Sources 76 (1998) 1-10.

[28] T. Xiang, J. Sunarso, W. Yang, Y. Yin, A.M. Glushenkov, L.H.Li, P.C.Howlett, Y. Chen, Ball milling: a green mechanochemical approach for synthesis of nitrogen doped carbon nanoparticles, Nanoscale 5 (2013) 7970-7976.

[29] B.M. Babić, S.K. Milonjić, M.J. Polovina, B.V. Kaluđerović, Point of zero charge and intrinsic equilibrium constants of activated carbon cloth, Carbon 37 (1999) 477-481.

[30] Lj. Matović, N. Vukelić, U. Jovanović, K. Kumrić, J. Krstić, B. Babić, A. Đukić, Mechanochemically improved surface properties of activated carbon cloth for the removal of As(V) from aqeuous solutions, Arab. J. Chem, in press, online 17 July 2016, doi.org/10.1016/j.arabjc.2016.07.004

[31] B.M. Babić, S.K. Milonjić, M.J. Polovina, S. Čupić, B.V. Kaluđerović, Adsorption of zinc, cadmium and mercury ions from aqueous solutions of an activated carbon cloth, Carbon 40 (2002) 1109-1115.

[32] S.J. Gregg, K.S.W. Sing, Adsorption, Surface Area and Porosity, Academic Press New York, 1967, p 124.

[33] J. Rouquerol, P. Llewellyn, and F. Rouquerol, Is the BET equation applicable to microporous adsorbents? In: Characterisation of porous solids VII. P. Llewellyn, F. Rodriguez-Reinoso, J. Rouquerol, and N. Seaton (Eds): Stud. Surf. Sci. Catal., 160 (2007) 49-56.

[34] M. M. Dubinin, Physical adsorption of gases and vapours in microspores, in Progress in Surface and Membrane Science, Vol. 9, Cadenhead D A, ed. (New York: Academic Press), 1975, p 1–70.

[35] G. Horvath, K. Kawazoe, Method for the Calculation of Effective Pore Size Distribution in Molecular Sieve Carbon, J. Chem. Eng. Jpn. 16 (1983) 470-475.

[36] S.L. Goertzen, K.D. Thériault, A.M. Oickle, A.C. Tarasuk, H. Andreas, Standardization of the Boehm titration. Part I. CO_2 expulsion and endpoint determination, Carbon 48 (2010) 1252–1261.

[37] S.J. Gregg, K.S.W. Sing, Adsorption, Surface Area and Porosity (Second Edition), vol. 41, Academic Press, London, New York, 1982.

[38] V Strelko Jr., D.J. Malik, M. Street, Characterisation of the surface of oxidised carbon adsorbents, Carbon, 40 (2002) 95-104.

[39] C. Sellitti, J.L. Koening, H, Ishida, Surface Characterization of graphitized carbon fibers by attenuated total reflection fourier transform infrared spectroscopy, Carbon, 28 (1990) 221-228.

[40] E. Paul, E. Fanning, and M. Albert Vannice, A drifts study of the formation of surface groups on carbon by oxidation, Carbon 31 (1993)721-730.

[41] M. Acik, G. Lee, C. Mattevi, A. Pirkle, R.M.Wallace, M. Chhowalla, K. Cho and Y. Chabal, The Role of Oxygen during Thermal Reduction of Graphene Oxide Studied by Infrared Absorption Spectroscopy, J. Phys. Chem. C, 115 (2011) 19761.

[42] S. Biniak, G. Szymański, J. Siedlewski, A Światkowski, The characterization of activated carbons with oxygen and nirogen surface groups , Carbon 35 (1997) 1799-1810.

[43] B. Saha, I.D. Harry, U. Siddiqui, Electrochemically Modified Viscose-Rayon-Based Activated Carbon Cloth for Competitive and Noncompetitive Sorption of Trace Cobalt and Lead Ions from Aqueous solution, Sep. Sci. Technol, 44 (2009) 3950-3972.

[44] J.-H. Zhou, Z.-J. Sui, J. Zhu, P. Li, D. Chen, Y.-C. Dai, W.-K. Yuan, Characterization of surface oxygen complexes on carbon nanofibers by TPD, XPS and FT-IR, Carbon 45 (2007) 785-796.

[45] J Chmiola, G Yushin, R Dash, Y Gogotsi, Effect of pore size and surface area of carbide derived carbons on specific capacitance, J Power Sources 158 (2006) 765–772

[46] G. Gryglewicz, J. Machnikowski, E. Lorenc-Grabowska, G.Lota, E. Frackowiak, Effect of pore size distribution of coal-based activated carbons on double layer capacitance, Electrochim Acta 50 (2005) 1197–1206

[47] S. Roldán, M. Granda, R. Menéndez, R. Santamaría, Mechanisms of Energy Storage in Carbon-Based Supercapacitors Modified with a Quinoid Redox-Active Electrolyte, J. Phys. Chem. C, 115 (2011) 17606-17611.

[48] A. Śliwak B Grzyb, J. Ćwikla, G.Gryglewicz, Influence of wet oxidation of herringbone carbon nanofibers on the pseudocapacitance effect, Carbon 64 (2013) 324-333.

[49] D.Hulicova-Jurcakova, M. Seredych, G.Q. Lu, T.J.Bandosz, Combined effect of nitrogen- and oxygen-containing functional groups of microporous activated carbon on its electrochemical performance in supercapacitors, Adv. Funct. Mater., 19 (2009) 435-447

[50] M. Pakula, S. Biniak, A.Swiatkowski, Changes in the Surface Chemistry and Adsorptive Properties of Active Carbon Previously Oxidised and Heat-treated at Various Temperatures. II. Electrochemical Investigations of Surface Chemistry, *Ads. Sci.Technol. 20 (2002) 583-593*

[51] Q. T. Qu, B. Wang, L.C. Yang, Y. Shi, S. Tian, Y.P. Wu, Study on electrochemical performance of activated carbon in aqueous Li_2SO_4, Na_2SO_4 and K_2SO_4 electrolytes, Electrochem. Commun. 10 (2008) 1652–1655

[52] V. Subbramian, C. Luo, A.M. Stephan, K.S. Nahm, S. Thomas, B. Wei, Supercapacitors from activated Carbon Derived from Banana Fibers. J. Phys. Chem. C. 111 (2007) 7527-7531.

[53] V. Dodevski, M. Puševac, M. Vujković, J. Krstć, S. Krstić, D. Bajuk-Bogdanović, B. Kuzmanović, B. Kaluđerović, S. Mentus, Complex insight into the chrge storage behavior of active carbons obtained by carbnization of the plane tree seed, Electrochim. Acta 222 (2016) 156-171.

[54] R. de Levie, L. Pospíšil, On the coupling of interfacial and diffusional impedances, and on the equivalent circuit of an electrochemical cell, J. Electroanal. Chem and Interf. Electrochem, 22 (1969) 277-290.

[55] A. Burke, R&D considerstion for the performance and application of electrochemical capacitors, Electrochim. Acta 53 (2007) 1083-1091.

[56] D. Sun, X. Yan, J. Lang, Q. Xue, High performance supercapacitor electrode based on graphene paper via flame-induced reduction of graphene oxide paper, J. Power Sources 222 (2013) 52-58.

[57] A. Jain, C. Xu, S. Jayaraman, R. Balasubramanian, J.Y. Lee, M. P. Srinivasan, Mesopous activated carbons with enhanced porosity by optimal hydrothermal pre-treatment of biomass for supercapacitor applications, Micropor Mesopor. Mater. 203 (2015) 178-185

[58] M. Olivares-Marín, J.A. Fernández, M.J. Lázaro, C. Fernández-González, A. Macías-García, V. Gómez-Serrano, F. Stoeckli, T.A. Centeno, Cherry stones as precursor of activated carbons for supercapacitors, Mater. Chem.Phys. 114 (2009) 323-327.

[59] H. Chen, J. Di, Y. Jin, M. Chen, J. Tian, Q. Li, Active carbon wrapped carbon nanotube buckypaper for the electrode of electrochemical supercapacitors, J. Power Sources 237 (2013) 325-331.

[60] X. Li, W. Xing, S. Zhuo, J. Zhou, F. Li, S.-Z. Qiao,G.-Q. Lu, Preparation of capacitor's electrode from sunflower seed shell, Bioresource. Technol. 102 (2) (2011) 1118e1123.

[61] T. Liu, T.V. Sreekumar, S. Kumar, R.H. Hauge, R.E. Smalley, Carbon 41 (2003) 2440-2442.

[62] X. Wang, R.S. Chandrabose, S.-E. Chun, T. Zhang, B. Evanko, High Enegy Density Aqeuous Electrochemical Capacitors with a KI-KOH electrolyte, ACS Appl. Mater. Inter. 2015, 7, 19978−19985.

[63] H. Peng, G. Ma, K. Sun, J. Mu, Z. Lei, One-step preparation of ultrathin nitrogen-doped carbon nanosheets with ultrahigh pore volume for high-performance supercapacitors, J. Mater. Chem. A 2 (2014) 17297-17301

[64] L. Chen, Z. Huang, H. Liang, W. Yao, Z. Yu and S. Yu, Flexible all-solid-state high-power supercapacitor fabricated with nitrogen-doped carbon nanofiber electrode material derived from bacterial cellulose, Energ. Environ. Sci., 2013, 6, 3331.

[65] Z. Wu, A. Winter, L. Chen, Y. Sun, A. Turchanin, X. Feng, K. Müllen, Three-Dimensional Nitrogen and Boron Co-doped Graphene for High-Performance All-Solid-State Supercapacitors, Adv. Mater., 2012, 24, 5130.

[66] J. Suárez-Guevara, V. Ruiz, P. Gomez-Romero, Hybrid energy storage: high voltage aquous supercapacitors based on activated carbon-phototungstate hybrid materials, J. Mater. Chem. A 2 (2014) 1014-1021.

[67] K. Sun, Q. Yang, Y. Zheng, G. Zhao, Y. Zhu, X. Zheng, G. Ma, High performance Symmetric Supercapacitor Based on Sunflower Marrow Cabon Electrode Material, *Int. J. Electrochem. Sci.,* 12 (2017) 2606 – 2617.

[68] N.S.M. Nor, M. Deraman, M. Suleman, M.R.M. Jasni, J.G. Manjunatha, M.A.R. Othman, S.A. Shamsudin, Supercapacitors using Binderless Activated Carbon Monoliths Electrodes consisting of a Graphite Additive and Percarbonized Biomass Fibers, *Int. J. Electrochem. Sci.,* 12 (2017) 2606 – 2617.

Figure captions

Fig.1. N_2 adsorption (colored symbol)/desorption (empty symbol) curves (a) and the pore size distribution (b) of ACC and ACCm samples
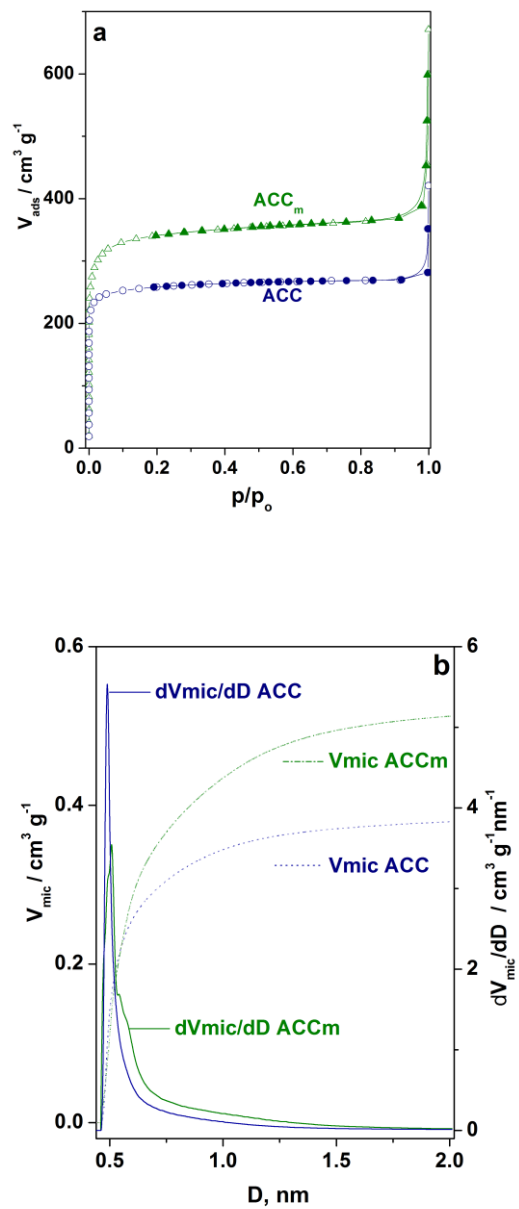
Fig.2. FTIR spectra of the samples (a), SEM picture of ACC (b), particle size distribution of ACCm (c) and SEM picture of ACCm sample (d).
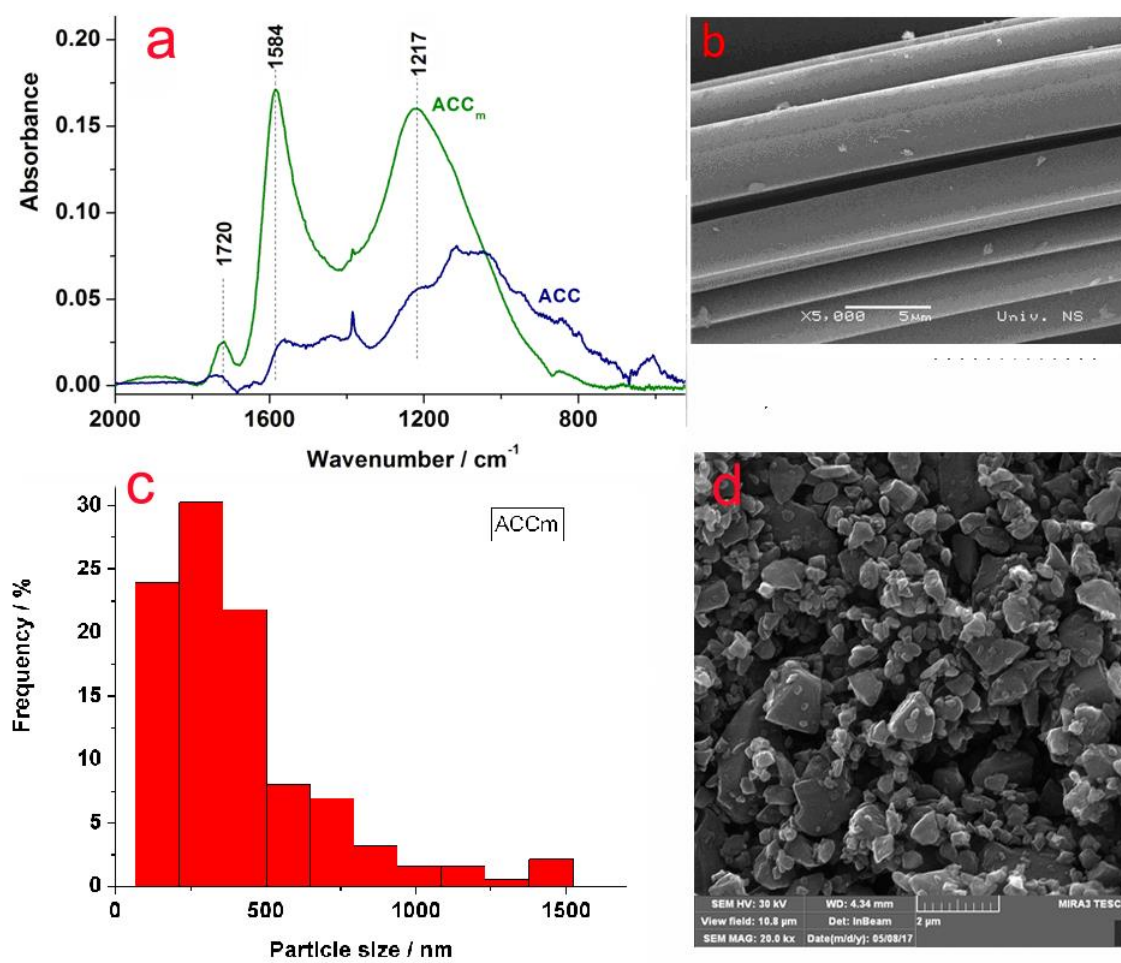
Fig.3. Cyclic Voltamograms of ACC (a-c) and ACCm (d-f) measured in three aqueous solutions.
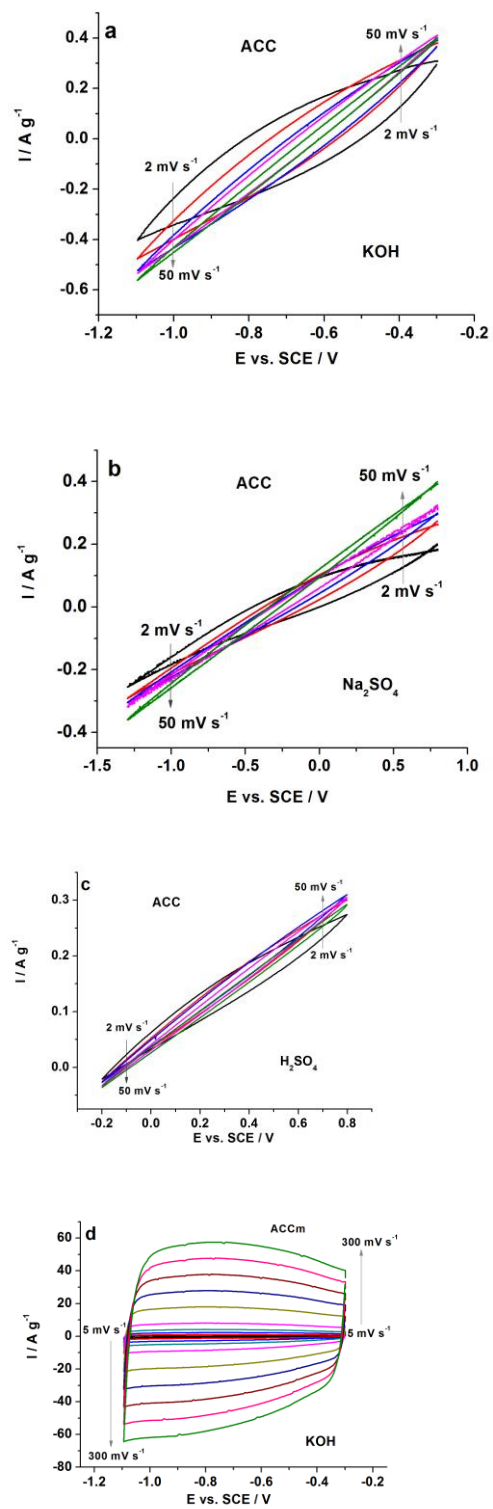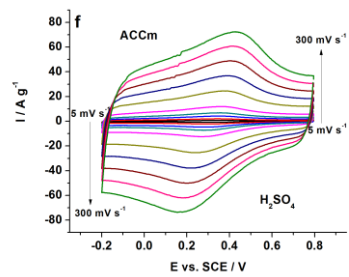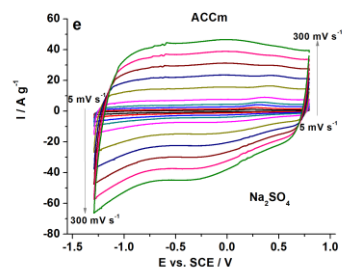
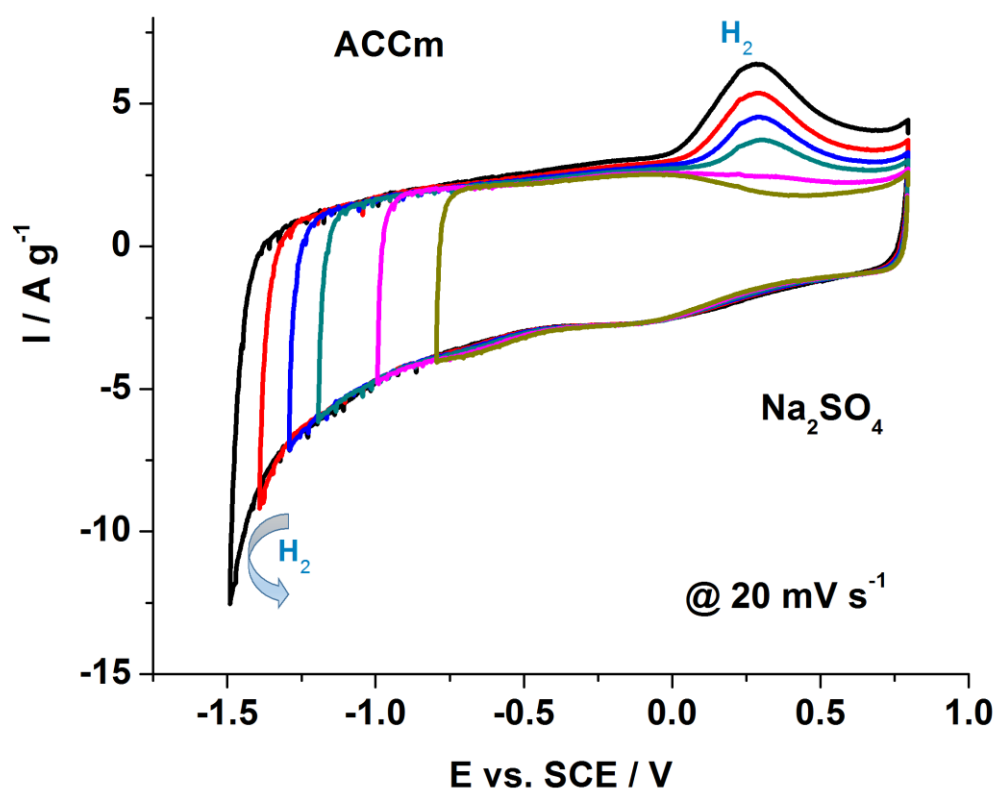**Fig.4.** CVs of ACCm measured in Na_2SO_4 at different potential intervals.

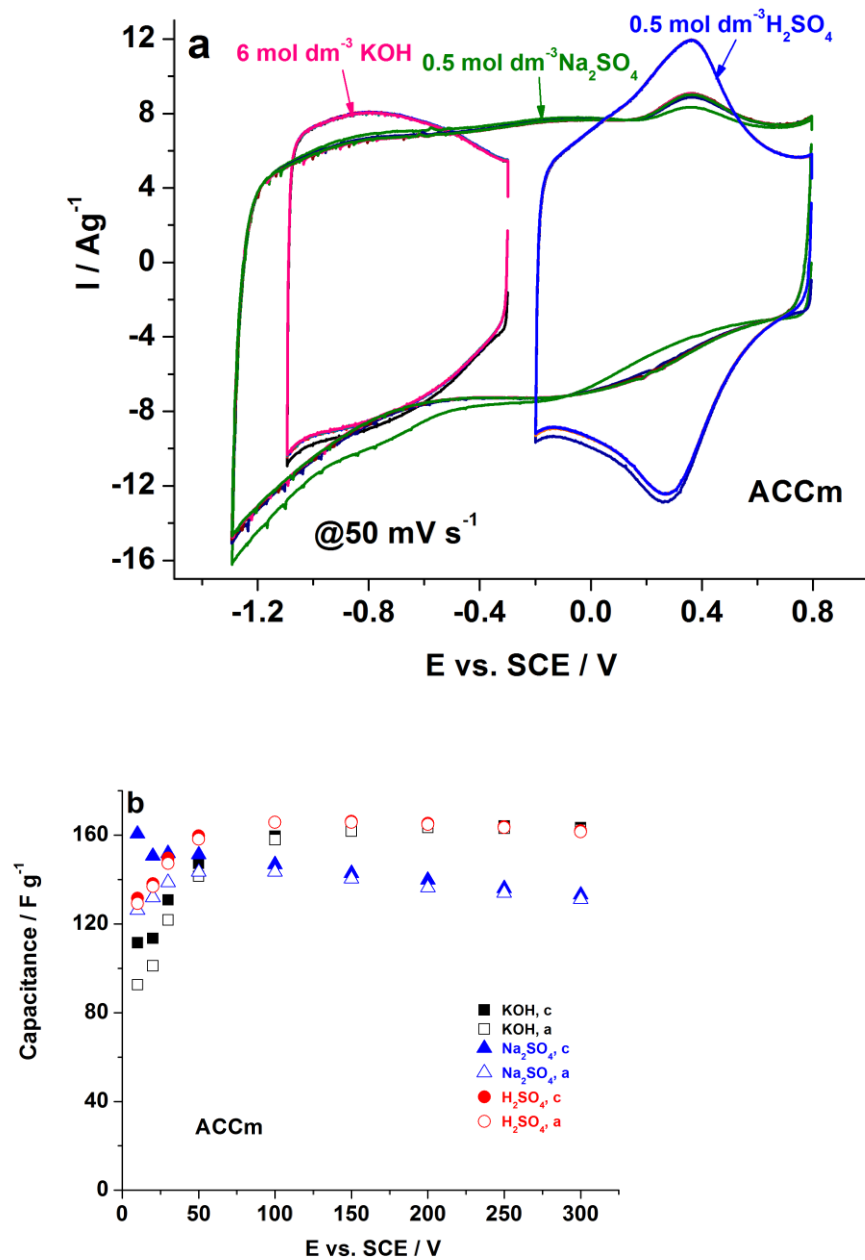**Fig.5.** Comparison of CVs (a) and specific capacitance (b) of ACCm in three different aqueous electrolytes.
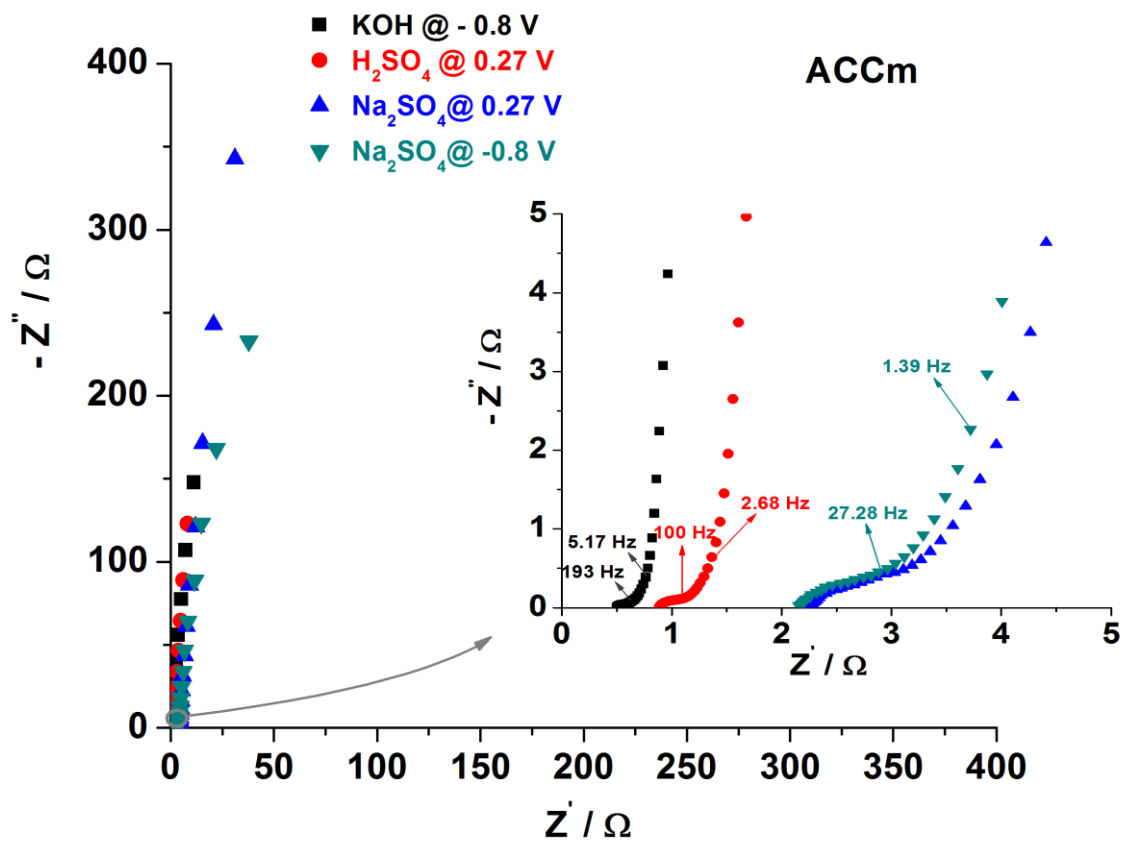
Fig.6. Nyquist diagrams of ACC$_m$ measured in KOH, H$_2$SO$_4$ and Na$_2$SO$_4$

Fig.7. a) Comparative CVs of AC [51] and ACCm (here) measured in KOH; b) CVs of ACCm measured in H_2SO_4 at various potential intervals. Scan rate was 20 mV s^{-1}.
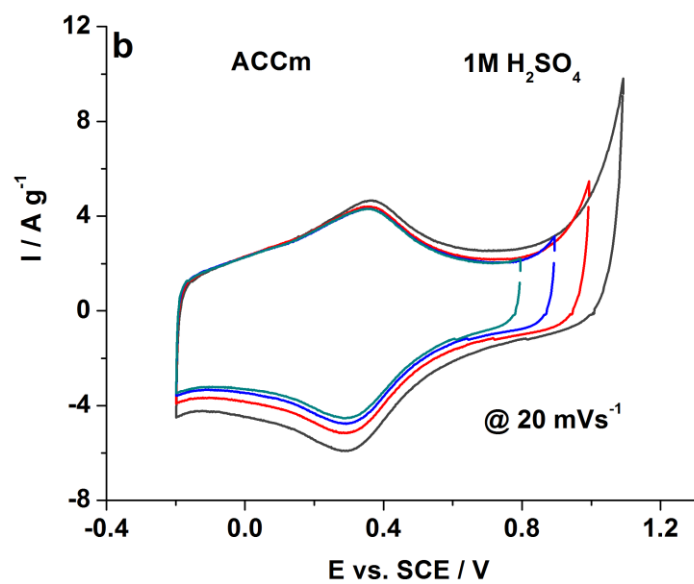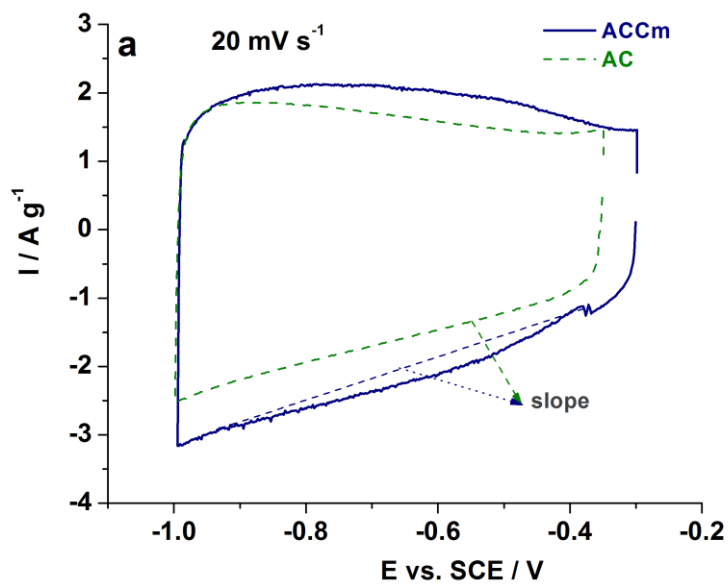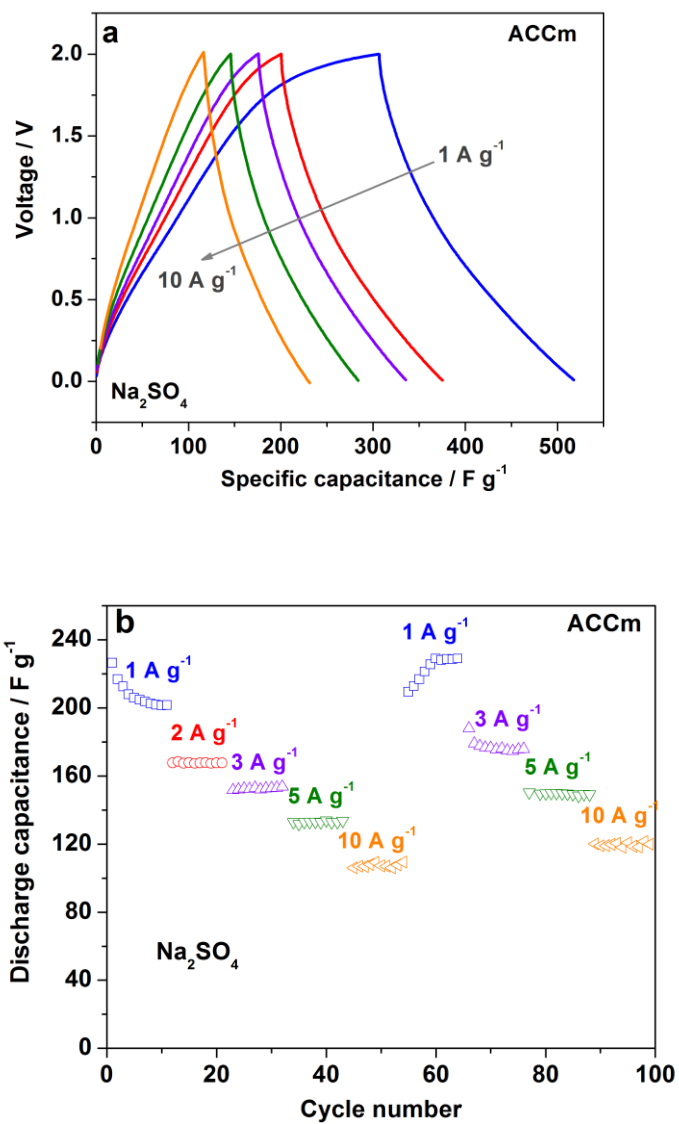
Fig.8. Charge/discharge curves (a,c) and specific capacitance (b) of ACCm at various current rates. Cyclic performance of ACCm at 10 A g^{-1} (d).
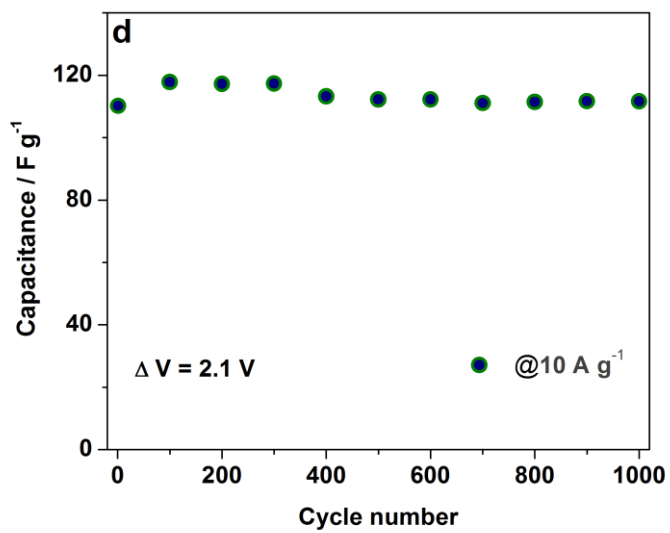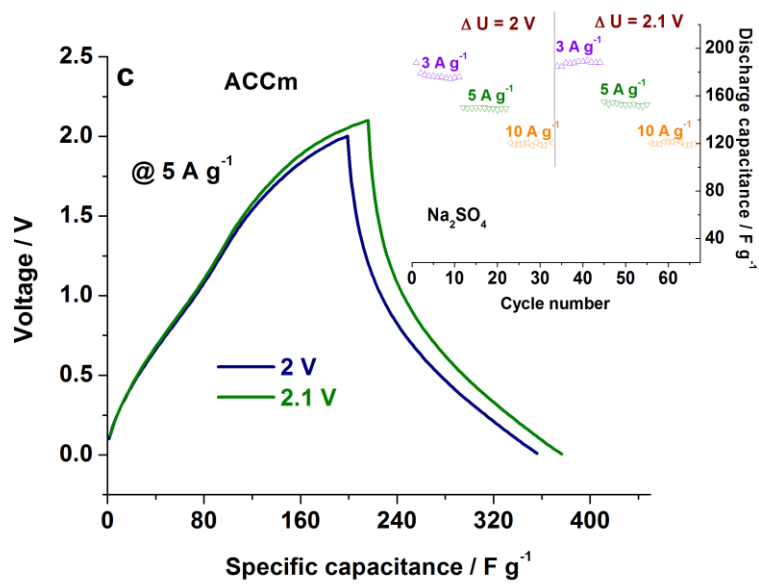
Table 1. Textural parameters of the samples.

Sample	S_{BET} / $m^2 g^{-1}$	V_{mic} / $cm^3 g^{-1}$			V_{tot} / $cm^3 g^{-1}$
		t-plot	HK	DR	
ACC	1028	0.392	0.379	0.395	0.424
ACCm	1340	0.529	0.513	0.509	0.586

Table 2. The amount of ACC and ACC$_m$ surface functional groups

Sample	Basic groups (mmol g^{-1})	Acidic groups (mmol g^{-1})	Carboxyl groups (mmol g^{-1})	Lactonic groups (mmol g^{-1})	Phenolic groups (mmol g^{-1})
ACC	0.2493	2.5093	0.1173	0.0074	2.3846
ACCm	0.7933	3.5313	0.1113	0.0094	3.4106

Table 3. The electrochemical performances of different carbon-based capacitors

Samples	Energy density / Wh kg^{-1}	Power Density / W kg^{-1}	Electrolyte	ΔU /V
Hydrochar-derived ACs [55]	7.6	4500	H_2SO_4	1
Cherry stones-derived ACs [56]	1-2 4-6	1500-2000 5500-6000	H_2SO_4 $(C_2H_5)_4NBF_4/CH_3CN$	0.8 2.0
Sunflower seed shell derived nanoporous carbon [58]	4.8	2400	KOH	/
Flower-like and hierarchical porous carbon (FHPC) [18]	15.9	317.5	Na_2SO_4	1.8
r-GO [54]	6.1 4.86	500.2 4998.9	KOH	1
CNT buckypaper/AC layer [57] Single-walled CNTs/AC [59]	9.6 1.6	4000	KOH	1
Carbon fibers [60]	7	6200	KOH-KI	1.6
Nitrogen-doped graphene-like carbon nanosheets [61]	20.8 13.3	225 5872	Na_2SO_4	1.8
Nitrogen-doped carbon nanofiber [62]	6.07	390.53	PVA-H_2SO_4 gel-electrolyte	1
Boron and Nitrogen co-doped graphene [63]	8.7	1650	PVA-H_2SO_4 gel-electrolyte	0.8
AC [64]	4.05	45000 (P_{max})	H_2SO_4	1
AC-PW$_{12}$ [64]	10.39 (C) 4.96 (C+PW$_{12}$)	115000 (P_{max})	H_2SO_4	1.6
Sunflower marrow derived porous carbon[65]	12.4	817	Na_2SO_4	2
Activated Carbon Monoliths Electrodes[66]	3.5	155	H_2SO_4	1
Mechanochemically[this work] activated carbon cloth (ACCm) this work	31.7 23.4 16.8	2000 5245 10497	Na_2SO_4	2-2.1